

Silica microlenses for extrinsic optical fibre sensors

Celia Gómez-Galdós^{a, b,*}, María Gabriela Fernández-Manteca^{a, b}, Borja García-García^{a, b}, Andrea Pérez-Asensio^{a, b}, José Francisco Algorri^{a, b, c}, José Miguel López-Higuera^{a, b, c}, Adolfo Cobo^{a, b, c}, and Luis Rodríguez-Cobo^{a, b, c}

^aPhotonics Engineering Group, Universidad de Cantabria (UC), 39005, Santander, Spain;

^bInstituto de Investigación Sanitaria Valdecilla (IDIVAL), 39011, Santander, Spain; ^cCIBER-bbn, Instituto de Salud Carlos III, 28029, Madrid, Spain;

ABSTRACT

Microlenses for extrinsic optical fibre sensors have been fabricated on fused silica using Ultrafast Laser-assisted Etching (ULAE) technique. Then the quality of a proof-of-concept manufactured microlens was evaluated by studying point-spread function profile and taking Airy disk as reference.

Keywords: ULAE, microlens, PSF

1. INTRODUCTION

For centuries, optical systems have been created for a variety of purposes, ranging from observing celestial bodies to magnifying tiny objects on Earth [1]. Moreover, many other optical systems with different applications are used. In any case, every image-forming system is improved until high-quality image is achieved. Aberrations, which refer to effects related to image distortion, are identified as a result. Consequently, processes aimed at minimizing aberrations are conducted. Accordingly, the process of evaluation optical systems includes the identification as assessment of aberrations [2]. For optical system diagnosis, a relevant effect is its response to a point source illumination [3]. In general, a blurred image through the optical system is related to a low-quality system and the spreading degree is a valid parameter for optical quality evaluation of the system. In particular, the image produced by an ideal optical system from a point source is well known and it is possible to identify aberrations on the optical system by comparing to this the image produced by the optical system from a point source. The objective of this study is to validate the microlenses manufactured on silica via Ultrafast Laser-Assisted Etching for extrinsic optical fibre sensors [4].

In this work, a proof-of-concept silica microlenses has been optically analysed using the Point Spread Function (PSF). The roughness obtained by the ULAE technique without post-processing techniques will determine the optical quality of the system, affecting its application to extrinsic fibre-optic sensors.

2. THEORETICAL CONCEPTS

2.1. Point Spread Function

The Point Spread Function (PSF) is defined as the optical field distribution when imaging a point source. Therefore, each optical system has its own PSF. In case of a perfect focusing optical system where optical geometry approach is considered, i.e. the image formation is solely based on ray tracing, when a point is taken as an object, the resulting image must also be a point. However, if wave optics is considered, also for a perfect focusing optical, a plane wave is transformed into a spherical converging wave. Then, the image of a point is more complex.

At least, in an ideal optical system, the image of a monochromatic point source is a shape with a central point surrounded by concentric disks, commonly referred to as an Airy pattern. This result is related to the diffraction limit effect and can be analytically explained using a Fraunhofer diffraction theory. The bright center of the pattern is named as the Airy disk, while the outer disks exhibit alternating dark and bright regions. These regions are associated with destructive and constructive diffraction interference, respectively. The pattern size depends on different setup conditions. When an optical system is just a focusing lens and a monochromatic point source is the object, the main factors are the lens f-number and the illumination wavelength. In conclusion, perfect systems are those that result in Airy disk as an image. Where the well-known solution is defined by the Bessel function of first order, J_1 , a mathematical special function whose independent

* ggaldosc@unican.es

variable is also a special parameter, τ , which corresponds to a fraction of image position, x , dependent of illumination wavelength (λ) and f-number of the optical system, F . In terms of the optical intensity of the image (I) and being I_0 the maximum intensity in the center

$$I = I_0 \left(\frac{2J_1(\tau)}{\tau} \right)^2 \quad \text{where } \tau = \frac{x\pi}{\lambda F} \quad (1)$$

However, when dealing with real configurations, it is necessary to take imperfections into account. In situations where aberrations occur finding a solution becomes more complex. Several studies have been carried out centered on different derived aberration contributions [5]. When conducting an analytical study on PSF in systems affected by spherical aberration, it was concluded that, as an approximation, the PSF can be represented as a linear combination of several Bessel functions of different order [6].

2.2. Lens design

Since spherical aberration is typically the major distortion factor in the design of a focusing lens, the lens is intentionally shaped with an aspheric form. Particularly, an aspheric lens of 1 mm diameter of fused silica is simulated using OpticStudio Zemax (version 22.2.1). It is a plano-convex type lens where curve geometry is described by Eq. 1. So, lens parameters are lens radius of curvature, r , the conic constant, k , and coefficients which describe lens deviation from a spherical surface, α_i .

$$z = \frac{r^2 / k}{1 + \sqrt{1 - (1+k)(r^2 / k)}} + \alpha_1 r^2 + \alpha_2 r^4 + \alpha_3 r^6 + \alpha_4 r^8 + \alpha_5 r^{10} + \alpha_6 r^{12} + \alpha_7 r^{14} + \alpha_8 r^{16} \quad (2)$$

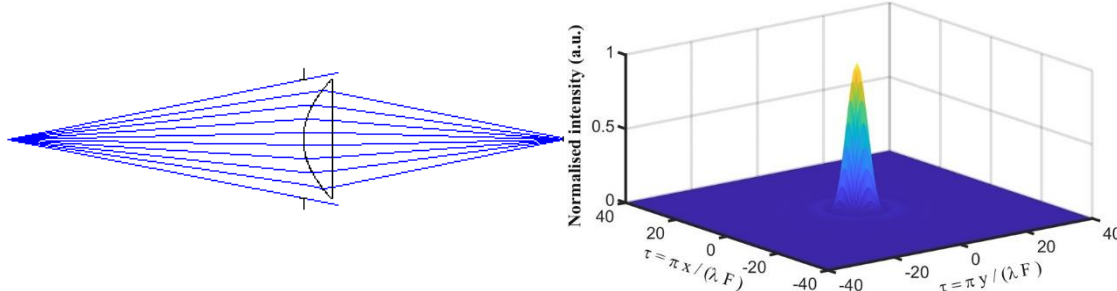


Figure 1. Cross-section image of the ray tracing of the optical system characterised by a point source ($\lambda = 637$ nm) and the aspheric lens under analysis, all performed in Zemax OpticsStudio software (left). PSF of the optical system when monochromatic point source, $\lambda = 637$ nm, illuminates the aspheric lens, obtained with Zemax OpticsStudio analysis tools (right).

Designed lens has parameters: $r = 0.9$ mm, $k = -1.25$ and $\alpha_i = 0$, except $\alpha_1 = 0.4$ (system of f-number 1.14). Assuming for simulation a monochromatic point source, $\lambda = 637$ nm, PSF is obtained by using software analysis tools (Fig. 1).

2.3. Analysis

For an ULAE-manufactured silica microlens, the optical field distribution of the point source image will differ from the Airy pattern. This is due to aberration effects expected from roughness. Methods to determine resolution of the optical system are required. Two main strategies are considered in related references: direct imaging or sub-diffraction size fluorescent microspheres imaging [7]. There exist a lot of reported techniques, algorithms, and protocols to evaluate optical systems imaging fluorescent microspheres, but there are few references about direct imaging measurements. In this work, direct imaging is the selected method. Consequently, images undergo signal processing in order to be compared to a reference result, which is the simulation of the point spread profile of the designed lens. Figure 2 shows (left side) that Airy disk diameter corresponds to the distance of nearest positions from the center where the Bessel function is cancelled out, i.e., those x such that $J_1(\tau) = 0$. Hence, it is considered that the resolution limit of the optical system will be set by central peak extremes. On the right side of Fig.2, the analysis demonstrates that the region defined as the Airy disk, determined by the limits of the central peak can be effectively approximated using Gaussian fit. In this case, the standard deviation of the Gaussian distribution becomes another parameter of interest

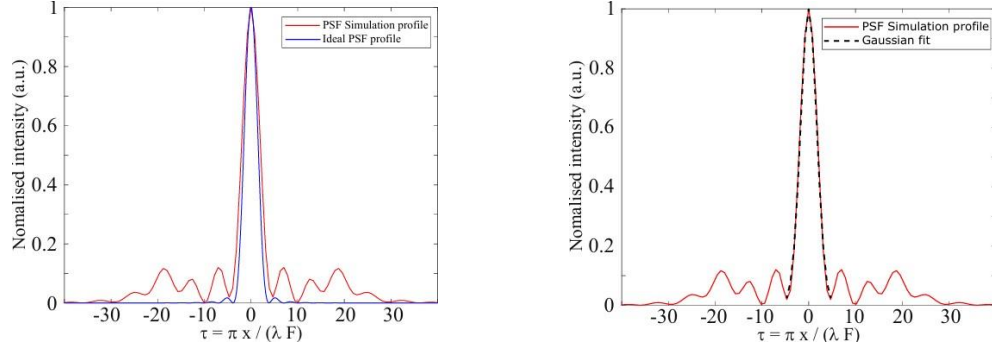


Figure 2. Point spread function profiles of the ideal optical system and simulation of the silica lens, blue and red lines respectively (left). Simulated PSF, in red line, and Gaussian fit with black dashed line (right).

3. EXPERIMENTAL ANALYSIS AND IMAGE PROCESSING

3.1. Lens manufacture

The lens fabrication process centres around ultrafast laser assisted etching [4]. In ultrafast laser processing, tightly focused ultra short pulses are used to induce nonlinear photoionisation in a dielectric substrate. The resulting modified substrate volume is highly localised so that material directly outside of the focal point is largely unaffected. One result of ULAE on a substrate is an increased etching rate (up to $\times 10^3$) when compared to pristine material [4]. Note that roughness this technique can reach root mean square values of 200 nm, while high-quality optical systems should range between 1 to 10 nm. For its manufacture, a commercial femtosecond fibre laser chirped pulse amplifier from Calmar laser was used (< 370 fs). It operates at 1030 nm, and the pulses are tightly focused into the 1 mm thick high purity fused silica glass using a 0.4 NA aspheric lens. The substrate was translated through laser focus using a motorised nanoresolution XYZ from Aerotech. In the subsequent etching process, the inscribed fused silica glass was immersed in a magnetically stirred etching solution of NaOH diluted with deionised water (5 wt%, 85°C). The etching time was 1 hour. It was empirically determined to facilitate easy release of the lens.

3.2. Experimental setup

The manufactured lens was mounted into a 3D printed plastic holder and attached to a movable stage. A 637 nm SM Fiber-Pigtailed Laser Diode of Thorlabs was mounted on an XYZ platform and aligned to convex side of the lens, providing an output spot of approximately of 4 μm in diameter at the connector output. At the plane side of the lens a OV5647 CCD sensor of 1.4 μm pixel size was aligned, with the capability of varying the distance from the lens. After an empirical sweep, the positions were established with a more clearly defined pattern, placing the source at $d_L \approx 3$ mm and the sensor at $d_S \approx 3$ mm from the lens surface

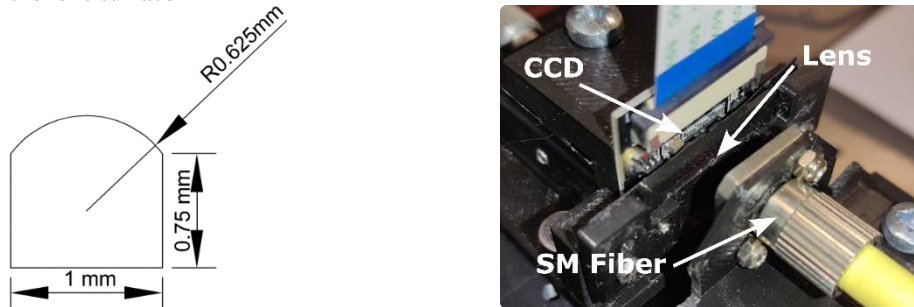


Figure 3. Top view of manufactured lens under analysis after etching (left). Experimental setup of SM fibre as monochromatic point source ($\lambda = 637$ nm), microlens on plastic holder and CCD sensor, all aligned (right)..

3.3. Results and analysis

During image acquisition two main considerations were considered. Firstly, the position if the CCD sensor was adjusted by varying lens-sensor distance to accurate measurements. Secondly, the laser power was carefully set to avoid saturated pixels. Consequently, imaging was performed at different positions for a given illumination intensity. This process resulted in multiple image stacks, allowing for qualitative determination of the focusing position by observing the plane image

displacement. This was particularly effective due to the short focal length of the ULAE-fabricated microlens, which was $f = 1.14$ mm. Once best-focused capture was selected from a stack of non-saturated images, depicted in Fig. 4 (right) the previously described Gaussian fitting was applied to analyse the selected image, which is shown in Fig. 4 (left). While qualitative spreading degree can be observed in that figure, quantitative results of spreading degree are presented in Table 1. The resolution limit in terms of the Airy diameter (d), as well as the standard deviation (σ), and their respective ratios to the ideal (d/d_{Airy} , $\sigma/\sigma_{\text{Airy}}$) and simulated (d/d_{simul} , $\sigma/\sigma_{\text{simul}}$) results are included. Both the diameter and standard deviation (σ) show a ratio of approximately 7 between measured and simulated profiles. In summary, the results indicate that the imaging quality of the ULAE-fabricated microlens is low. However, considering the absence of post-processing in manufacturing, these results show a promising level of improvement, particularly in terms of roughness.

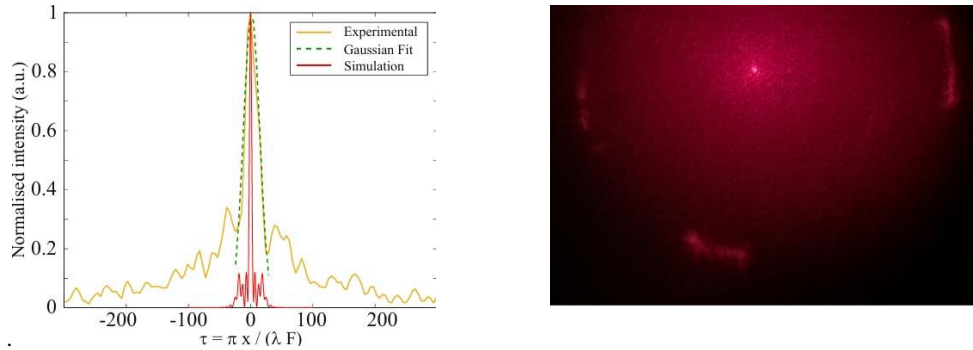


Figure 4. PSF simulation, red line, and experimental, orange line, profiles of silica micro-lens. Gaussian fitting for experimental postprocessing results, dashed green (left). CCD capture corresponded to the experimental data profile (right).

4. CONCLUSIONS

In this work, a proof-of-concept lens has been fabricated using ULAE for extrinsic fibre optic sensors. Although the shape obtained corresponds to the initial simulated design, the roughness obtained is not of sufficient quality to focus light as verified by PSF analysis. The results obtained, although insufficient for a practical application, lay the foundation for possible microlens systems as long as the finishes are improved with post-processing techniques to reduce lens roughness.

ACKNOWLEDGEMENTS

This work was supported by the R+D projects INNVAL23/10, and INNVAL24-28, funded by Instituto de Investigación Marqués de Valdecilla (IDIVAL); C.G-G acknowledges Concepcion Arenal predoctoral fellow and J.F.A. thanks RYC2022-035279-I, funded by MCIN/AEI/10.13039/501100011033 and FSE+; TED2021-130378B-C21, funded by MCIN/AEI/10.13039/501100011033 and European Union NextGenerationEU/PRTR; PID2022-137269OB-C22, funded by MCIN/AEI/10.13039/501100011033 and FEDER, UE; Plan Nacional de I+D+i and Instituto de Salud Carlos III (ISCIII), Subdirección General de Redes y Centros de Investigación Cooperativa, Ministerio de Ciencia, Innovación y Universidades, through CIBER-BBN (CB16/01/00430) and CIBERINFEC (CB21/13/00068), co-financed by the European Regional Development Fund “A way to achieve Europe”.

REFERENCES

- [1] A Davies, R. and Kasper, M. Adaptive optics for Astronomy. *Annual Review of Astronomy and Astrophysics*, 50(1), 305–351 (2012). <https://doi.org/10.1146/annurev-astro-081811-125447>
- [2] Wyant, J. C. Basic Wavefront Aberration Theory for Optical Metrology. In *Applied Optics and optical engineering* (pp. 1–64). Essay (1992), Academic Press.
- [3] Braat, J. J. M., van Haver, S., Janssen, A. J. E. M., and; Dirksen, P. (2008). Chapter 6 assessment of optical systems by means of point-spread functions. *Progress in Optics*, 349–468. [https://doi.org/10.1016/s0079-6638\(07-51006-1](https://doi.org/10.1016/s0079-6638(07-51006-1)
- [4] Ochoa, M., Roldan-Varona, P., Algorri, J., Lopez-Higuera, J. & Rodriguez-Cobo, L. Polarisation-independent ultrafast laser selective etching processing in fused silica. *Lab On A Chip*. 23, 1752–1757 (2023)
- [5] Mahajan, V. N. Optical aberrations. (1998). *Optical Imaging and Aberrations*, 139–202. <https://doi.org/10.1117/3.265735.ch3>
- [6] Mik's, A., and Nov'ak, J. (2019). Point spread function of an optical system with defocus and spherical aberration analytical formulas. *Applied Optics*, 58(21), 5823. <https://doi.org/10.1364/ao.58.005823>
- [7] Metz, J., Gintoli, M., and; Corbett, A. (2022). Fully Automated Point Spread Function Analysis Using Pycalibrate. <https://doi.org/10.1101/2022.10.11.511725>
- [8] Marasco, A., Massari, D., Neichel, B., Schreiber, L., and; Wizinowich, P. (2020). Review of PSF reconstruction methods and application to post-processing. *Adaptive Optics Systems VII*. <https://doi.org/10.1117/12.2560805>